From balance to imbalance: a shift in the dynamic behaviour of Chhota Shigri glacier, western Himalaya, India

M. F. Azam, P. Wagnon, A.L. Ramanathan, Christian Vincent, Parmanand Sharma, Y. Arnaud, Anurag Linda, J. G. Pottakkal, P. Chevallier, V. B. Singh, et al.

From balance to imbalance: a shift in the dynamic behaviour of Chhota Shigri Glacier (Western Himalaya, India)

Mohd. Farooq AZAM[1], Patrick WAGNON[2], Alagappan RAMANATHAN[1], Christian VINCENT[3], Parmanand SHARMA[1], Yves ARNAUD[2], Anurag LINDA[1], Jose George POTTAKKAL[1], Pierre CHEVALLIER[4], Virendra Bahadur SINGH[1], Etienne BERTHIER[5].

[1] School of Environmental Sciences, Jawaharlal Nehru University, New Delhi 110067, India

[2] IRD / UJF - Grenoble 1 / CNRS / G-INP, LGGE UMR 5183, LTHE UMR 5564, Grenoble, F-38402, France.

[3] UJF - Grenoble1 / CNRS, Laboratoire de Glaciologie et Géophysique de l'Environnement (LGGE) UMR 5183, Grenoble, F-38041, France.

[4] Laboratoire Hydrosciences (UMR 5569 – CNRS, IRD, Montpellier Universities 1&2), CC57, Université Montpellier 2, 34095 Montpellier Cedex 5, France

[5] LEGOS, CNRS, Université de Toulouse, 14 av. Edouard Belin, 31400 Toulouse, France.

Corresponding author:

Patrick WAGNON

patrick@lgge.obs.ujf-grenoble.fr

Revised for the *Journal of Glaciology*.

Abstract

Mass-balance and dynamic behaviour of Chhota Shigri Glacier have been investigated between 2002 and 2010 and compared to data collected in 1987/1989. During the period 2002/2010, the glacier experienced a negative glacier-wide mass balance of –0.67 ± 0.40 m water equivalent per year (w.e. yr^{-1}). Between 2003 and 2010, elevation and ice flow velocities are slowly decreasing in the ablation area leading to a 24 to 37% reduction in ice fluxes, an expected response of the glacier dynamics to its recent negative mass balances. The reduced ice fluxes still remain far larger than the balance fluxes calculated from the year 2002 to 2010 average surface mass balances. Therefore, further slow down, thinning and terminus retreat of Chhota Shigri Glacier are expected over the next years. Conversely, the 2003/2004 ice fluxes are in good agreement with ice fluxes calculated assuming that the glacier-wide mass balance is zero. Given the limited velocity change between 1987/1989 and 2003/2004 and the small terminus change between 1988 and 2010, we suggest that the glacier has experienced a period of near zero or slightly positive mass balance in the 1990s, before shifting to a strong imbalance in the 21st century. This result challenges the generally accepted idea that glaciers of Western Himalaya have been shrinking rapidly for the last decades.

1. Introduction

Although Himalayan glaciers have important social and economic impacts (e.g. Barnett and others, 2005), they have never been monitored on a long-term basis and little is known about recent glacier trends or their contribution to local and regional water supplies, even giving rise to

47 a controversial statement in the IPCC 4th assessment report saying that "the likelihood of them
48 disappearing by the year 2035 or perhaps sooner is very high if the Earth keeps warming at the
49 current rate" (Cogley and others, 2010). A general negative mass balance of mountain glaciers
50 on a global level is clearly revealed from recent research (e.g. Cogley, 2009; Zemp and others,
51 2009) but the effect of global warming in the Himalaya is still under debate (Yadav and others,
52 2004; Roy and Balling, 2005). Though temperate glacial mass-balance change is one of the best
53 indicators of climate change (Oerlemans, 2001; Vincent and others, 2004; Ohmura and others,
54 2007) the paucity of mass-balance data in Himalaya makes it difficult to obtain a coherent
55 picture of regional climate change impacts in this region. In the Indian Himalaya the first mass-
56 balance study started on Gara Glacier (Himachal Pradesh) in September 1974 (Raina and others,
57 1977) and ended in 1983 (Dobhal and others, 2008). According to Dyurgerov and Meier (2005),
58 eight glaciers in the Indian Himalaya were surveyed for mass balance at least for one year during
59 the 1980s. Unfortunately each study was restricted to short periods, not more than one decade
60 (Dobhal and others, 2008). Remote sensing studies were also attempted in this part of Himalaya,
61 but these studies either deal with only surface area changes (e.g. Kulkarni and others, 2007;
62 Bhambri and others, 2011) or cover short periods (Kulkarni, 1992; Berthier and others, 2007).

63

64 The present study is based on mass balance and surface ice flow velocity measurements
65 conducted on Chhota Shigri Glacier, Himachal Pradesh, India between 2002 and 2010, and on a
66 comparison to data collected in 1987/1989. In the Indian Himalaya, this is one of the longest
67 continuous field mass-balance dataset. Moreover, in October 2009, a Ground Penetrating Radar
68 (GPR) survey was also conducted to measure ice thickness. Eight years of mass-balance
69 measurements, surface ice velocities and ice thickness data provide an opportunity to study the

behaviour of this glacier. The main objectives of this paper are (i) to present the recent mass balance of Chhota Shigri Glacier, (ii) to determine the ice fluxes at five cross sections from thickness and ice velocities, and (iii) to compare these data with the ice fluxes inferred from cumulative surface mass balance upstream of the same cross sections. These results give insights into the mass-balance trend of the glacier over the last two to three decades, and allow us to assess whether it is in equilibrium with the climate of the 21st century.

2. Site description and methodology

2.1 Site description

Chhota Shigri Glacier (32.2^{o} N and 77.5^{o} E) is a valley-type glacier located in the Chandra-Bhaga River basin of Lahaul and Spiti Valley, Pir Panjal Range, Western Himalaya. This glacier extends from 6263 m to ~4050 m a.s.l., is ~9 km long and covers 15.7 km^2 of area. The snout of this glacier is easy to locate from one year to another because it is well defined, lying in a narrow valley and giving birth to a single proglacial stream. The main orientation of this glacier is north except for its tributaries which have a variety of orientations (Fig. 1). The lower ablation area (<4400 m a.s.l.) is partly covered by debris representing ~3.4% of the total surface area. This glacier is located in the monsoon-arid transition zone and is influenced by two atmospheric circulation systems: the Indian monsoon during summer (July–September) and the northern-hemisphere mid-latitude westerlies during winter (January–April) (Singh and others, 1997; Bookhagen and Burbank, 2006; Gardelle and others, 2011).

2.2 Mass balance

The first series of mass-balance measurements was performed on Chhota Shigri Glacier between 1987 and 1989 (Nizampurkar and Rao, 1992; Dobhal and others, 1995; Kumar, 1999). The bedrock topography and surface ice velocity were also surveyed over the same period by gravimetric and stake displacement methods respectively (Dobhal and others, 1995; Kumar, 1999). We re-initiated the mass-balance observations in 2002. From that year, annual surface mass-balance measurements have been carried out continuously on Chhota Shigri Glacier at the end of September or beginning of October using the direct glaciological method (Paterson, 1994). Ablation was measured through a network of ~22 stakes distributed between 4300 and 5000 m a.s.l. (Fig. 1) whereas in the accumulation area, the net annual accumulation was obtained at six sites (by drilling cores or pits) between 5100 and 5550 m a.s.l. (Wagnon and others, 2007). In the accumulation area, the number of sampled sites is limited due to the difficulty in access and high elevation. The glacier-wide mass balance, B_a is calculated according to:

$$B_a = \sum b_i (s_i / S) \quad (1)$$

Where b_i stands for the mass balance of the altitudinal range (m w.e. yr^{-1}), i, of map area s_i and S symbolizes the total glacier area. For each altitudinal range, b_i is obtained from the corresponding stake readings or net accumulation measurements.

2.3 Surface velocity

Annual surface ice velocities were measured at the end of each ablation season (September-October) by determining the annual stake displacements (~22 stakes) using a Differential Global Positioning System (DGPS). These geodetic measurements were performed in kinematic mode relative to two fixed reference points outside the glacier on firm rocks. The accuracy in x (easting), y (northing) and z (elevation) of each stake position is estimated at ±0.2 m depending mainly on the size of the hole in which the stake has been set-up. Thus the surface ice velocities measured from stake displacements have an accuracy of ±0.3 m yr^{-1}.

2.4 Ice thickness

Ground penetrating radar measurements were conducted in October 2009 to determine ice thickness on five transverse cross sections (Fig. 1) between 4400 and 4900 m a.s.l. A pulse radar system (Icefield Instruments, Canada) based on the Narod transmitter (Narod and Clarke, 1994) with separate transmitter and receiver, was used in this study with a frequency centered near 4.2 MHz and antenna length of 10 m. Transmitter and receiver were towed in snow sledges along the transverse profile, separated by a fixed distance of 20 meters, and used to record measurements every 10 m. The positions of the receiver and the transmitter are known through DGPS measurements, within an accuracy of ±0.1 m. The speed of electromagnetic wave propagation in ice has been assumed to be 167 m μs^{-1} (Hubbard and Glasser, 2005). The field measurements were performed in such a way as to obtain reflections from the glacier bed located more or less in the vertical plane with the measurement points at the glacier surface, allowing the determination of the glacier bed in two dimensions. The surface of the bedrock was constructed as an envelope of all ellipse functions, which give all the possible reflection positions between

sending and receiving antennae. Ice thickness was measured along four transverse profiles (profiles 1-4) on the main glacier trunk and one (profile 5) on a western tributary (Fig. 1).

3. Data analysis and results

3.1 Glacier-wide mass balance and mass-balance profile

The annual glacier-wide mass balance and cumulative mass balance of Chhota Shigri Glacier between 2002 and 2010 are plotted in Figure 2. The glacier-wide mass balance was negative except for three years (2004/2005; 2008/2009 and 2009/2010). It varies from a minimum value of –1.40 m w.e. in 2002/2003 to a maximum value of +0.33 m w.e. in 2009/2010. The cumulative mass balance of Chhota Shigri is -5.37 m w.e. between 2002 and 2010 while the glacier-wide mass balance averaged over the same period is –0.67 m w.e. yr^{-1}.

The quantitative uncertainty associated with the glaciological mass balance requires a distinction between the accumulation zone and the ablation zone. In the accumulation zone, the surface mass-balance measurements were obtained from shallow boreholes (auger). Therefore, they are based on core length and density determination. In the ablation zone, the measurements have been carried out from ablation stakes. The overall error (standard deviation) on point measurements are estimated at 0.30 m w.e. and 0.15 m w.e. in the accumulation zone and in the ablation zone, respectively. The overall error comes from a variance analysis (Thibert and others; 2008) applied to all types of errors (ice/snow density, core length, stake height determination, liquid-water content of the snow, snow height). Although conducted on a glacier in the Alps, the analysis of Thibert and others (2008) can be generalized to other glaciers because it is based on

159 measurement errors which are similar on every glacier when using the glaciological method.
160 However, only 6 sites are sampled in the accumulation zone (11.6 km²), and 22 sites in the
161 ablation zone (4.1 km²). The uncaptured spatial variability of surface mass balance may cause
162 systematic errors on the glacier-wide mass balance. In the accumulation zone, the spatial
163 variability remains unknown and is probably very high as observed for other glaciers (e.g.
164 Machguth and others, 2006). In the ablation zone, stakes set up at the same altitude show similar
165 values except on the terminal tongue which is debris covered (0.54 km²). Consequently, the
166 overall uncertainties on mass-balance profile have been assessed at 0.5 m w.e. in the
167 accumulation zone, 0.25 m w.e. in the white ablation zone and 0.5 m w.e. in the debris covered
168 area of the glacier. Moreover, the surface area estimation also causes systematic error. The
169 uncertainty on the surface area calculated for each altitudinal range is estimated at 5%.
170 Combining these errors at different altitudinal ranges using Equation (1), the uncertainty on the
171 annual glacier-wide mass balance is 0.4 m w.e. yr^{-1}. As revealed by other studies (e.g. Vincent,
172 2002; Thibert and others, 2008; Huss and others, 2009), this estimation confirms that the
173 glaciological method needs to be calibrated by a volumetric method over a long period of
174 monitoring (i.e. >5 years) in order to limit the systematic errors and to improve the accuracy of
175 absolute values of mass balance. Note that the uncertainty of relative changes in mass balance
176 from year to year is smaller than those inherent in annual mass balances, given that the influence
177 of systematic errors can be reduced.
178
179 We also calculated the mass-balance profile between 2002 and 2010 (Fig. 3). For each
180 altitudinal range, we computed the average of all available measurements. Figure 3 reveals that
181 melting in the lowest part of the ablation area (below 4400 m a.s.l.) is reduced by about 1 m w.e.

182 yr^{-1} irrespective to its altitude. This is due to the debris cover (~5 to 10 cm thick debris mixed
183 with isolated rocks) which reduces the melting in this region (Mattson and others, 1993; Wagnon
184 and others, 2007). Moreover the lower part of Chhota Shigri Glacier flows in a north-south
185 oriented deep and narrow valley (Fig. 1), causing the glacier tongue to receive less solar
186 radiation due to the shading effect of the steep valley slopes.
187

188 **3.2 Ice thicknesses and cross section areas**

189 Thanks to clear reflections, ice-bedrock interface was generally easy to determine on all
190 profiles. Figure 4 provides an example of the radargram obtained at cross section 2. A radar wave
191 velocity of 167 m μs^{-1} was used for calculations of ice thickness at all the profiles. The cross
192 sections obtained from GPR measurements reveal a valley shape with maximum ice thickness
193 greater than 250 m (Fig. 5). The centerline ice thickness increases from 124 m at 4400 m a.s.l.
194 (cross section 1 in Fig. 1) to 270 m at 4900 m a.s.l. (cross section 4), which confirms that the
195 thicknesses obtained by gravimetric methods in 1989 (Dobhal and others, 1995), twice lower
196 than the present results, were under-estimated as proposed by Wagnon and others (2007). The
197 cross sectional areas are given in Table 1. The accuracy of the calculated ice thickness is
198 determined, in part, by the accuracy of the measurement of the time delays and the antenna
199 spacing. Additional errors may arise because the smooth envelope of the reflection ellipses is
200 only a minimal profile for a deep valley-shape bed topography, with the result that the ellipse
201 equation will be governed by arrivals from reflectors located toward the side and thus not
202 directly beneath the points of observation. Further errors may be introduced by assuming that all
203 reflection points lie in the plane of the profile rather than on an ellipsoid. No errors associated to
204 radar wave velocity variations between snow and ice have been accounted for because all cross

sections were surveyed in the ablation zone or slightly above (with the firn-ice transition depth at the surface or < 2 m deep). Hence, the radar wave velocity for ice (167 m μs^{-1}) was used to calculate all ice depths. The overall uncertainty in ice thickness is estimated as ±15 m. Given that the uncertainty in ice surface coordinates is low (±0.1 m), the uncertainty on cross section areas mainly arises from the uncertainty in ice thickness. The uncertainties in cross section areas are 16, 9, 10, 10 and 15% for the cross sections 1, 2, 3, 4 and 5 respectively.

3.3 Ice velocity

Annual surface ice velocities were also measured between 2002 and 2010. However, some data gaps exist due to discontinuous DGPS signal, or loss of stakes. The ice velocities from 2003/2004 were used in this study because they provided the most complete dataset (Fig. 6). The center line horizontal ice velocities at each cross section were calculated by linear interpolation method along the center line between the velocities measured immediately upstream and downstream of the cross section (ablation stakes visible on Fig. 1). Mean cross section velocities are required to compute the ice fluxes (see section below). A map of the surface ice velocity field has been derived by correlating 2.5-m SPOT5 images acquired on 13 November 2004 and 21 September 2005 (Berthier and others, 2005). Comparison of the satellite-derived velocities with 16 nearly simultaneous DGPS velocity measurements shows a mean difference of 0.2 m yr^{-1} and a standard deviation of 1.6 m yr^{-1}. The ratio between the center line horizontal velocity and the mean surface velocity (all extracted from the satellite-derived 2004/2005 velocity field) was found to be 0.80 and 0.78 for cross sections 2 and 3 respectively. Reliable velocity measurements could not be measured from SPOT5 imagery for other cross sections. Using the mean value of

227 0.79, the mean horizontal velocity has been calculated from the center line velocity for each gate
228 cross section (Table 1).
229
230 **3.4 Ice fluxes from kinematic method**
231 The ice flux Q (m^3 of ice per year) through each cross section was calculated using the
232 cross sectional area S_c (m^2) and depth-averaged horizontal ice velocity U (m yr^{-1}).
233
234 $$Q = U S_c \qquad (2)$$
235
236 The depth-averaged horizontal ice velocity was derived from the mean surface ice velocity
237 calculated in the previous section. Nye (1965) gives ratios of depth-averaged horizontal ice
238 velocity to mean surface ice velocity varying from 0.8 (no sliding) to 1 (maximum sliding). Here,
239 we assume a mean basal sliding, with a constant ratio of 0.9. The calculated ice fluxes and
240 maximum depth at each cross section are given in Table 1. The flux through cross section 3 at
241 4750 m a.s.l. is higher than the flux through cross section 4 at 4900 m a.s.l. This is due to the ice
242 influx from the western part of the glacier (flux through cross section 5) which contributes to
243 cross section 3 and not to cross section 4 (Fig. 1).
244
245 The largest uncertainty on the depth-averaged horizontal ice velocity results from the
246 ratio between the depth velocity and the surface flow velocity. The estimated factor 0.9 and
247 unknown variations in the basal sliding lead to an uncertainty of roughly ±10% in the calculated
248 flux, which lies within the range of uncertainty of the other variables as discussed by Huss and
249 others (2007). Consequently, we can assess that depth-averaged horizontal ice velocity at each

cross section is known with an accuracy of 1.0 to 3.0 m yr^{-1} depending on the cross sections. Combining these errors on the cross sectional area and mean velocity, the uncertainties on the ice fluxes are 0.21, 0.69, 0.92, 0.89 and 0.38 x 10^6 m^3 yr^{-1} for the cross sections 1, 2, 3, 4 and 5 respectively. Here we have considered that the errors are systematic, so these uncertainties are probably over-estimated.

3.5 Ice fluxes obtained from surface mass balance

We also calculated ice fluxes using annual surface mass balance measured during 2002/2010. Although the dynamic changes are neglected here, this method allows us to estimate the ice fluxes for each section from mass-balance data according to the following equation:

$$Q = \frac{1}{0.9} \sum_{z}^{z\max} b_i s_i \qquad (3)$$

Where Q is the ice flux (converted into m^3 of ice per year using an ice density of 900 kg m^{-3}, hence the factor 1/0.9) at a given elevation, z, and b_i is the annual mass balance of the altitudinal range i of map area s_i. The altitudinal ranges taken into account in the calculation are located between z and the highest range of the glacier z_{max} (highest altitude of the glacier area contributing ice to the cross section). We assume here that on each point of the glacier above this altitude, z, the surface elevation has remained unchanged from one year to the next.

The ice fluxes calculated from annual mass-balance data at the 5 cross sections each year are given in Table 3, while the average ice fluxes for the eight years are given in Figure 7. The

uncertainties on ice fluxes resulting from surface mass balance are directly derived from the mass-balance uncertainties (see section 3.1) applied to areas contributing to each cross section.

4. Discussion

The first and main objective of this section is to discuss the mass-balance change of Chhota Shigri Glacier over the last two to three decades using not only direct mass-balance observations (over the last eight years) but also ice-flux analysis. The second goal is to give insights into the specific dynamics and the future retreat of this glacier that can be expected in relation to its recent surface mass balance (hereafter referred to as SMB).

4.1 Null to slightly positive mass balance during the 1990s inferred from ice fluxes

The ice fluxes obtained from the kinematic method using ice thickness and 2003/2004 ice velocities are much higher than the average fluxes derived from the 2002/2010 SMBs, the latter being often negative (Table 2). Thus in this section, to assess the mean state of the glacier corresponding to the ice fluxes obtained by the kinematic method, we compare these measured ice fluxes to theoretical ice fluxes calculated from SMB assuming the glacier to be in steady state. The glacier-wide mass balance obtained by the glaciological method is -0.67 m w.e. yr^{-1} over the 2002/2010 period. Consequently, the SMB needs to be increased by 0.67 m w.e. yr^{-1}, for the glacier to be in steady state with the present surface area. For each year (2002/2010), we calculated the theoretical ice flux from SMB at each cross section assuming the glacier was in steady state. For this purpose, every year, a theoretical SMB at each elevation has been calculated by substracting the overall annual specific SMB of the same year. For instance, year 2002/2003 was characterized by a negative annual glacier-wide SMB of -1.40 m w.e. so we

295 calculated a new SMB profile by adding +1.40 m w.e. to the SMB at each elevation. In contrast
296 year 2009/2010 was characterized by a positive annual glacier-wide SMB of +0.33 m w.e. so we
297 calculated a new SMB profile by subtracting 0.33 m w.e. from the SMB at each elevation. The
298 resulting ice fluxes are reported in Table 3, together with the mean ice flux at each cross section
299 over the eight years and the corresponding standard deviations.
300
301 These ice fluxes are close to the 2003/2004 ice fluxes obtained by the kinematic method
302 (Fig. 7) indicating that the dynamic behaviour of the glacier in 2003/2004 is representative for
303 steady-state conditions. This suggests that in the years preceding 2003/2004, the glacier-wide
304 mass balance of this glacier has probably been close to zero and that, in 2003/2004, the ice fluxes
305 had not adjusted to previous year negative SMB.
306
307 This result is also supported by other observations. First, the ice velocities measured in
308 1987/1988 (Dobhal and others, 1995) are very close to the 2003/2004 values (Fig. 6) suggesting
309 that the dynamic behaviour of this glacier did not change a lot between 1988 and 2004. Second,
310 the terminus fluctuation measured between 1988 and 2010 show a moderate retreat equal to 155
311 m, equivalent to only 7 m yr^{-1}, in agreement with conditions not far from steady state. Given that
312 Berthier and others (2007) observed a glacier-wide SMB of Chhota Shigri Glacier of
313 approximately -1 m w.e. yr^{-1} during the period 1999 to 2004, the glacier is likely to have
314 experienced a null to slightly positive mass balance between 1988 and the end of the 20^{th}
315 century.
316
317

318 **4.2 Glacier dynamics starting to adjust to 21st century negative SMB**

319 In theory, the response of ice fluxes to surface mass balance is immediate (Cuffey and
320 Paterson, 2010, p. 468) but observations show a 1-5 year delay (Vincent and others, 2000; Span
321 and Kuhn, 2003; Vincent and others, 2009). For instance, Span and Kuhn (2003) found
322 synchronous decrease in ice velocity between eight glaciers in the Alps, which are driven by the
323 same mass-balance changes (Vincent and others, 2005). Consequently, the recent dynamic
324 behaviour of Chhota Shigri Glacier should be affected by the negative mass balance since 1999.
325 However, the stake network on Chhota Shigri Glacier, originally designed for SMB
326 measurements, is not best suited to accurately compare either the ice velocities or the thickness
327 variations because the measurements have not been performed exactly at the same location every
328 year and they are mainly restricted to the ablation area.
329
330 In spite of the above limitation, an attempt has been made to compare ice velocities and
331 elevations from the available stake network. For this purpose, stakes measured at the beginning
332 and at the end of the series have been selected on five short longitudinal cross sections (A, B, C,
333 D and E in Fig.1) along the center line of the glacier where the network is most dense. The
334 elevations in 2003 and 2010 and the ice velocities in 2003/2004 and 2009/2010 have been
335 reported on these longitudinal cross sections to deduce thickness and velocity changes in the
336 ablation area (Fig. 8, Table 4). Although the accuracy of the results is affected by the distance
337 between the point measurements, we can conclude that the part of the glacier below 4750 m a.s.l.
338 is in strong recession. First, the thickness has decreased annually by 0.7 to 1.1 m yr^{-1} over the last
339 seven years. Second, the ice velocities have been reduced by ~7 m yr^{-1} between 2003 and 2010
340 resulting in a 24 to 37% decrease in the ice fluxes since 2003. Despite an improvable monitoring

network, it may be surmised that the ice fluxes have been affected by the negative glacier-wide mass balance during (at least) the last eight years, and the dynamics of this glacier are progressively adjusting to the negative SMB. Consequently, we expect an accelerated terminus retreat in the coming years. If the SMB remained equal to its 2002/2010 average value in the future, the terminus would retreat by 5.6 km to reach an altitude of 4870 m a.s.l. (altitude where the ice flux is equal to zero) (Table 2).

5. Conclusion

The Chhota Shigri Glacier experienced negative mass balance over the 2002/2010 period. The glacier-wide mass balance of the glacier is estimated at –0.67 m w.e. yr^{-1} between 2002 and 2010, revealing strong unsteady-state conditions over this period. Conversely, ice fluxes calculated through 5 transverse cross sections by the kinematic method correspond to near steady-state conditions before 2004. Given that ice velocities measured in 2003/2004 are close to those measured in 1988, and that terminus has retreated only 155 m between 1988 and 2010, it seems that the dynamic change was moderate between 1988 and 2004. Therefore, considering that Berthier and others (2007) observed a negative glacier-wide mass balance of about -1 m w.e. yr^{-1} between 1999 and 2004 using satellite images, our analysis suggests that the glacier experienced a period of slightly positive or close to zero mass balance at the end of the 20^{th} century, before starting to shrink. As Chhota Shigri seems to be representative of other glaciers in the Pir Panjal Range (Berthier and others, 2007), it is possible that many Western Himalayan glaciers of northern India experienced growth during the last 10-12 years of the 20^{th} century, before starting to shrink at the beginning of the 21^{st} century.

Since 2003, ice velocities and elevation are decreasing in the ablation area. Our data suggest that the ice fluxes have diminished by 24 to 37% below 4750 m a.s.l. between 2003 and 2010. Even if we account for a 37% decrease in ice fluxes calculated from 2003/2004 ice velocities to obtain present ice fluxes values, it remains a very large imbalance with ice fluxes coming from glacier-wide mass balance of the last eight years. Thus the present dynamics (thickness and ice velocities) of this glacier are far from surface mass balance and climate conditions of the last eight years, even if it is progressively adjusting. Therefore the glacier is likely to undergo accelerated retreat in the near future.

This glacier is almost free of debris and thus its mass-balance variations are closely related to climate changes. This glacier has the longest running series of mass balance measurements in the Himalaya range. In the future, the dynamic behaviour and the mass balance need more detailed investigations, although such field measurements are demanding due to the very high altitude. In order to investigate the annual thickness and the ice velocity changes, we recommend performing elevation and ice velocity measurements on ~12 cross sections including some in the accumulation zone. We also recommend measuring the ice velocities from a dense network of stakes to be set up on longitudinal center lines in order to compare the annual velocity changes at the same points. Finally, we recommend calibrating and checking the mass-balance field measurements from a volumetric method (from photogrammetry or remote sensing techniques).

Acknowledgements

This work has been supported by the IFCPAR/CEFIPRA under the project n°3900-W1 and by the French Service d'Observation GLACIOCLIM as well as the Department of Science and Technology (DST), and Space Application Centre, Government of India. The French National Research Agency through ANR-09-CEP-005-01/PAPRIKA provided DGPS devices to perform field measurements. We thank J. E. Sicart, J. P. Chazarin, our field assistant Mr. B. B. Adhikari and the porters who have been involved in successive field trips, sometimes in harsh conditions. We would also like to thank Dr D. P. Dobhal for his kind cooperation in answering our queries regarding the earlier research on Chhota Shigri Glacier. E. Berthier acknowledges support from the French Space Agency (CNES) through the TOSCA and ISIS proposal #0507/786 and from the Programme National de Télédétection Spatiale (PNTS). We thank Jawaharlal Nehru University for providing all the facilities to carry out this work. Prof. K. A. Brugger and another anonymous reviewer have provided constructive suggestions and comments which helped to significantly improve the manuscript. They are greatly acknowledged here.

References

Barnett, T.P., J.C. Adam and D.P. Lettenmaier. 2005. Potential impacts of a warming climate on water availability in snow-dominated regions. *Nature,* **438**(7066), 303–309.

Berthier, E., H. Vadon, D. Baratoux, Y. Arnaud, C. Vincent, K. L. Feigl, F. Remy, and B. Legresy. 2005. Surface motion of mountain glaciers derived from satellite optical imagery. *Remote Sens. Environ.*, **95**(1), 14-28.

Berthier, E., Y. Arnaud, R. Kumar, S. Ahmad, P. Wagnon and P. Chevallier. 2007. Remote sensing estimates of glacier mass balances in the Himachal Pradesh (Western Himalaya, India). *Remote Sens. Environ.,* **108**(3), 327–338.

Bhambri, R., T. Bolch, R. K. Chaujar and S. C. Kulshreshtha. 2011. Glacier changes in the Garhwal Himalayas, India 1968-2006 based on remote sensing. *J. Glaciol.*, **57**(203): 543-556.

Bookhagen, B. and D.W. Burbank. 2006. Topography, relief, and TRMM-derived rainfall variations along the Himalaya. *Geophys.Res. Lett.,* **33**(8), L08405. (10.1029/2006GL026037).

Cogley, J. G. 2009. Geodetic and direct mass-balance measurements: comparison and joint analysis. *Ann. Glaciol.*, **50**(50), 96-100.

Cogley, J.G., J.S. Kargel, G. Kaser and C.J. Van der veen. 2010. Tracking the Source of Glacier Misinformation. *Science*, **327,** 522.

Cuffey, K.M. and W.S.B. Paterson. 2010. *The Physics of Glaciers*, fourth edition, Butterworth-Heinemann, *Elsevier,* 468.

Dobhal, D.P., S. Kumar and A.K. Mundepi. 1995. Morphology and glacier dynamics studies in monsoon–arid transition zone: an example from Chhota Shigri glacier, Himachal Himalaya, India. *Current Sci.,* **68**(9), 936–944.

Dohbal, D.P., J.G. Gergan and R.J. Thayyen. 2008. Mass balance studies of the Dokriani Glacier from 1992 to 2000, Garhwal Himalaya, India. *Bull. Glaciol. Res.,* **25,** 9-17.

Dyurgerov, M.B. and M.F. Meier. 2005. Glaciers and the changing Earth System: a 2004 snapshot. Boulder, CO, Institute of *Arctic and Alpine Research*. Ocassional Paper 58.

Gardelle, J., Y. Arnaud and E. Berthier. 2011. Contrasted evolution of glacial lakes along the Hindu Kush Himalaya mountain range between 1990 and 2009. *Global Planet. Change,* **75**(1-2), 47-55.

Hubbard B. and N. Glasser. 2005. *Field Techniques in Glaciology and Glacial Geomorphology*, Wiley & Sons Ltd, Chichester, England, 400 pp.

Huss, M., S. Sugiyama, A. Bauder and M. Funk. 2007. Retreat scenarios of Unteraargletscher, Switzerland, using a combined ice-flow mass-balance model. *Arctic, Antarc. Alp. Res.*, **39** (3), 422-431.

Huss, M., A. Bauder and M. Funk. 2009. Homogenization of long-term mass-balance time series. *Ann. of Glaciol.*, **50**, 198-206.

IPCC. 2007. Summary for Policymakers in Climate Change 2007: The Physical Science Basis. Contribution of Working Group I to the Fourth Assessment Report of the Intergovernmental Panel on Climate Change [Solomon, S., & others (eds.)]. *Cambridge University Press, Cambridge, United Kingdom and New York, NY, USA.*

Kulkarni, A.V. 1992. Mass balance of Himalayan glaciers using AAR and ELA methods. *J. Glaciol.*, **38**, 101-104.

Kulkarni, A.V. and 6 others. 2007. Glacial retreat in Himalaya using Indian remote sensing satellite data. *Current Sci.*, **92**(1), 69–74.

Kumar, S. 1999. Chhota Shigri Glacier: its kinematic effects over the valley environment, in the northwest Himalaya. *Current Sci.*, **77**(4), 594–598.

Machguth, H., O. Eisen, F. Paul and M. Hoelzle. 2006. Strong spatial variability of snow accumulation observed with helicopter-borne GPR on two adjacent Alpine glaciers. *Geophys. Res. Lett.*, **33**, L13503. (10.1029/2006GL026576.)

Mattson, L. E., J. S. Gardner and G. J. Young. 1993. Ablation on debris covered glacier, Punjab, Himalaya. *IAHS Publ.*, **218**, 289-296.

454 Narod, B.B. and G.K.C. Clarke. 1994. Miniature high-power impulse transmitter for radio-echo
455 sounding. *J. Glaciol*., **40**(134), 190-194.

456 Nijampurkar, V.N. and D.K. Rao. 1992. Accumulation and flow rates of ice on Chhota Shigri
457 Glacier, central Himalaya, using radio-active and stable isotopes. *J. Glaciol.*, **38**(128), 43–
458 50.

459 Nye, J.F. 1965. The flow of a glacier in a channel of rectangular, elliptic or parabolic cross
460 section. *J. Glaciol*., **5**(41), 661-690.

461 Oerlemans, J. 2001. *Glaciers and climate change.* Lisse, etc., A.A. Balkema, Brookfield, Vt.

462 Ohmura, A., A. Bauder, H. Mu¨ ller and G. Kappenberger. 2007. Long-term change of mass
463 balance and the role of radiation. *Ann. Glaciol.*, **46**, 367–374.

464 Paterson, W.S.B. 1994. *The physics of glaciers. Third edition*. Oxford, etc., Elsevier.

465 Raina, V.K., M.K. Kaul and S. Singh. 1977. Mass balance studies of Gara Glacier. *J. Glaciol*.
466 **18**(80), 415-423.

467 Roy, S.S. and R.C. Balling. 2005. Analysis of trends in maximum and minimum temperature,
468 diurnal temperature range, and cloud cover over India. *Geophys. Res. Lett.,* **32**(12),
469 L12702. (10.1029/2004GL022201.)

470 Singh P., S.K. Jain and N. Kumar. 1997. Estimation of snow and glacier-melt contribution to the
471 Chenab river, Western Himalaya, *Mount. Res. Dev.* **17**(1), 49-56.
472 (10.1029/2004GL022201.)

473 Span, N. and M. Kuhn. 2003. Simulating annual glacier flow with a linear reservoir model. *J.*
474 *Geophys. Res.*, **108**(D10), 4313. (10.1029/2002JD002828.)

475 Thibert, E., R. Blanc, C. Vincent and N. Eckert. 2008. Glaciological and volumetric mass-
476 balance measurements: error analysis over 51 years for Glacier de Sarennes, French Alps.
477 *J. Glaciol.,* **54**(186), 522–532.

478 Vincent, C. 2002. Influence of climate change over the 20th century on four French glacier mass
479 balances. *J. Geophys. Res.,* **107**(D19), 4375. (10.1029/2001JD000832.)

480 Vincent, C., M. Vallon, L. Reynaud and E. Le Meur. 2000. Dynamic behaviour analysis of
481 glacier de Saint Sorlin, France, from 40 years of observations, 1957–97. *J. Glaciol.*,
482 **46**(154), 499–506.

483 Vincent, C., G. Kappenberger, F. Valla, A. Bauder, M. Funk and E. Le Meur. 2004. Ice ablation
484 as evidence of climate change in the Alps over the 20th century. *J. Geophys. Res.*,
485 **109**(D10), D10104. (10.1029/2003JD003857.)

486 Vincent, C., E. Le Meur, D. Six and M. Funk. 2005. Solving the paradox of the end of the Little
487 Ice Age in the Alps. *Geophys. Res. Lett.,* **32**(9), L09706. (10.1029/2005GL022552.)

488 Vincent, C., A. Soruco, D. Six and E. Le Meur. 2009. Glacier thickening and decay analysis
489 from 50 years of glaciological observations performed on Glacier d'Argentière, Mont
490 Blanc area, France. *Ann. Glaciol.*. **50,** 73-79.

491 Wagnon, P., A. Linda, Y. Arnaud, R. Kumar, P. Sharma, C. Vincent, G. J. Pottakkal, E. Berthier,
492 Al. Ramanathan, S. I. Hasnain and P. Chevallier. 2007. Four years of mass balance on
493 Chhota Shigri Glacier, Himachal Pradesh, India, A New Benchmark Glacier In the Western
494 Himalaya. *J. Glaciol.,* **53**(183), 603-610.

495 Yadav, R.R., W.K. Park, J. Singh and B. Dubey. 2004. Do the western Himalayas defy global
496 warming? *Geophys. Res. Lett.,* **31**(17), L17201. (10.1029/2004GL020201.)

Zemp, M., M. Hoezle and W. Haeberli. 2009. Six decades of glacier mass-balance observations: a review of worldwide monitoring network. *Ann. Glaciol.*, **50**(50), 101-111.

Table and figure captions

Table 1: Calculated ice flux, mean surface ice velocity and maximum ice depth at each cross section. The mean surface horizontal ice velocities are from DGPS measurements performed in 2003/2004. The satellite-derived mean ice velocities are from the correlation of satellite images acquired on 13 November 2004 and 21 September 2005 (NA: Not available).

Table 2: Ice fluxes (in 10^6 m^3 ice yr^{-1}), inferred at each cross section from annual mass-balance data.

Table 3: Ice fluxes (in 10^6 m^3 ice yr^{-1}), obtained at every cross section, using steady state mass-balance assumption for every surveyed year.

Table 4: Thickness and surface velocity changes between 2003 and 2010 on 5 longitudinal cross sections (NA: Not available).

Figure 1: Map of Chhota Shigri Glacier with the measured transverse cross-sections (lines 1 to 5), the ablation stakes (dots) and the accumulation sites (squares). Also shown are longitudinal sections (lines A-E) used to calculate thickness and ice velocity variations (see section 4.2). The map (contour lines, glacier delineation) was constructed using a stereoscopic pair of SPOT5 (Systeme Pour l'Observation de la Terre) images acquired 12 and 13 November 2004 and 20 and 21 September 2005 (Wagnon and others, 2007). The map coordinates are in the UTM43 (north) WGS84 reference system.

Figure 2: Cumulative (line) and annual glacier-wide mass balances (histograms) of Chhota Shigri Glacier during 2002/2010.

Figure 3: The 2002/2010 average mass-balance profile and the hypsometry of Chhota Shigri Glacier. Altitudinal ranges are of 50 m (for instance, 4400 stands for the range 4400-4450 m, except for 4250 and 5400 which stand for 4050-4300 m and 5400-6250 m respectively).

Figure 4: Radargram of cross section 2: radar signals plotted side by side from west to east in their true spatial relationship to each other (interval between each signal of 10 m). The x-axis gives the amplitude of each signal (50 mV per graduation); the y-axis is the double-time interval (μs).

Figure 5: Ice depth and surface topography of cross-sections 1-5. The horizontal and vertical scales are the same for all cross-sections. All cross sections are oriented from west to east except cross section 5 which is north-south oriented.

Figure 6: Measured ice velocities plotted as a function of the distance from the 2010 terminus position. Measurements were collected along the central flow line.

Figure 7: Ice fluxes at every cross section derived (i) from 2003/2004 ice velocities and section areas (open squares) and (ii) from mass balance method for a glacier-wide SMB = 0 m w.e. (plain squares) or a glacier-wide SMB = -0.67 m w.e. (triangles). The error range for mass balance fluxes calculated from the mass balance method assuming a steady state (±1 standard deviation: hyphenes) is also given.

Figure 8: Elevation (dots) and surface ice velocity (triangles) between 2003 (continuous lines) and 2010 (dashed lines) along the longitudinal sections A, B, C, D and E shown in Figure 1.

Cross section	Altitude (m a.s.l.)	Area (10^4 m^2)	Mean surface ice- velocity from field data (m yr^{-1}) (central line velocity*0.79)	Satellite-derived mean surface velocities (m yr^{-1})	Ice flux (10^6 m^3 yr^{-1})	Max. depth at center of cross section (m)
1	4400	4.23±0.68	20.3	NA	0.78 ±0.21	124
2	4650	12.14±1.09	31.2	30.7	3.41 ±0.69	240
3	4750	16.49±1.65	29.2	29.2	4.35 ±0.92	245
4	4900	15.53±1.55	30.1	NA	4.20 ±0.89	270
5	4850	6.01±0.90	27.1	25.5	1.47 ±0.38	175

Table 1

Cross section	**Altitude (m a.s.l)**	**Hydrological years (October – September)**								**Mean**
		2002/03	**2003/04**	**2004/05**	**2005/06**	**2006/07**	**2007/08**	**2008/09**	**2009/10**	**2002/10**
Snout	4050	-22.26	-19.28	2.27	-22.21	-15.59	-14.65	2.06	5.24	-10.55
1	4400	-22.83	-19.55	3.78	-22.65	-15.43	-14.82	3.19	6.84	-10.18
2	4670	-14.31	-11.49	6.57	-14.35	-8.63	-8.21	6.03	8.70	-4.46
3	4735	-9.88	-7.68	6.89	-10.04	-5.45	-5.46	6.16	8.43	-2.13
4	4900	-1.41	-1.36	4.84	-2.30	0.05	-0.16	4.14	5.72	1.19
5	4870	-1.61	-1.30	2.08	-2.19	-0.57	-0.82	1.86	2.80	0.03

Table 2

Cross section	**Altitude (m a.s.l)**	**Hydrological years (October – September)**								**Mean**	**STD***
		2002/03	**2003/04**	**2004/05**	**2005/06**	**2006/07**	**2007/08**	**2008/09**	**2009/10**	**2002/10**	
Snout	4050	0.00	0.00	0.00	0.00	0.00	0.00	0.00	0.00	0.00	0
1	4400	1.25	1.32	1.33	1.38	1.43	1.03	0.96	1.17	1.23	0.17
2	4670	5.07	5.30	4.59	4.99	4.94	4.55	4.24	4.14	4.73	0.41
3	4735	6.04	6.11	5.27	5.85	5.70	5.02	4.69	4.68	5.42	0.58
4	4900	5.78	4.87	4.11	4.88	5.09	4.58	3.48	4.02	4.60	0.72
5	4870	2.76	2.48	1.63	2.17	2.49	2.06	1.46	1.77	2.10	0.46

*STD = standard deviation.

Table 3

Longitudinal section	Elevation change (m)	Velocity change (m yr^{-1})
A	-5.3	-6.6
B	-8.6	-8.8
C	-7.5	-7.4
D	-2.8	NA
E	-5.6	+4.8

Table 4

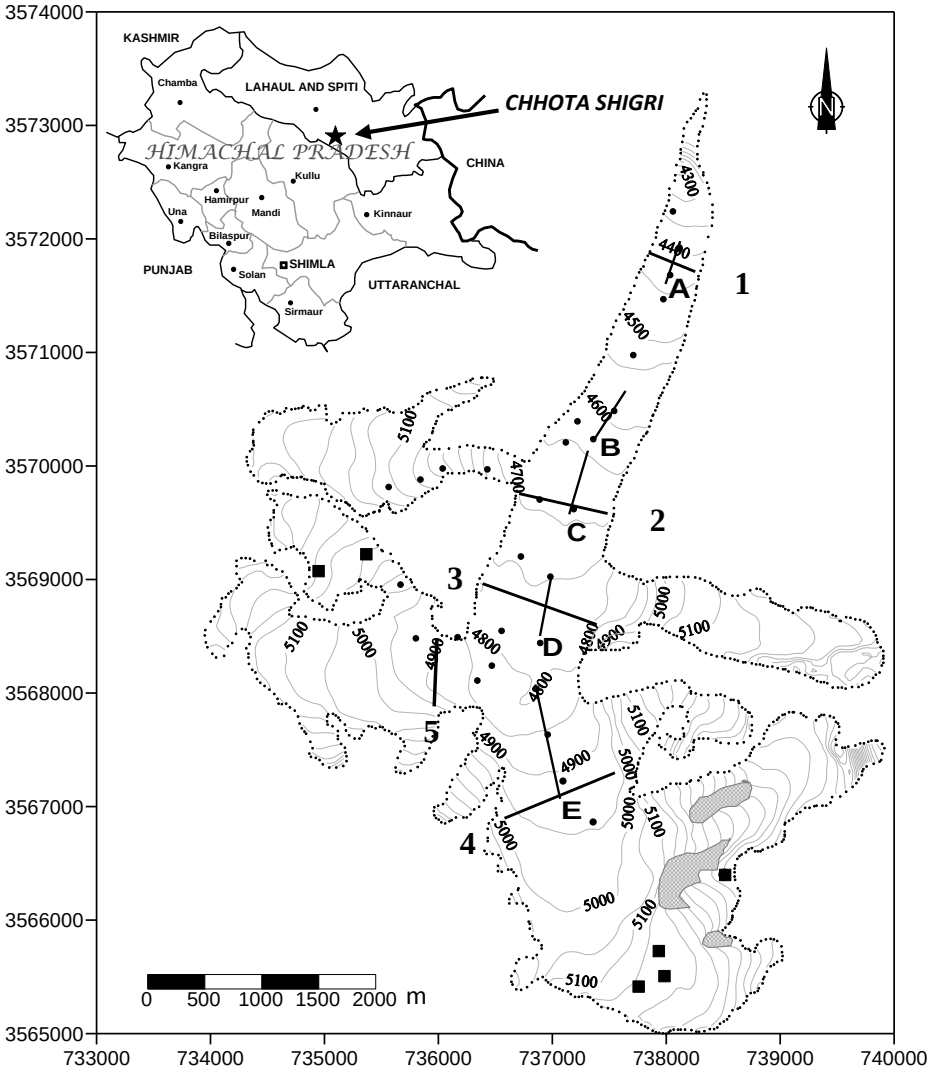

Figure 1

556

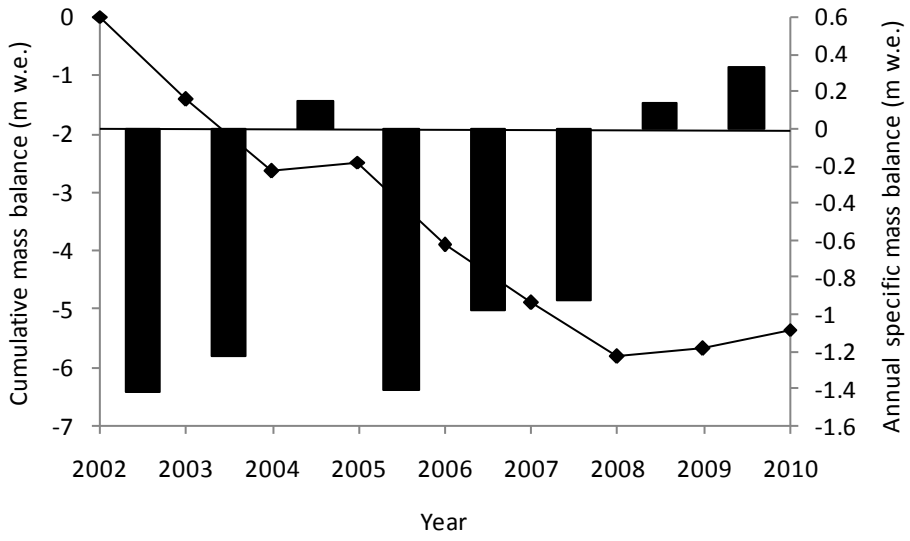

557

558 Figure 2

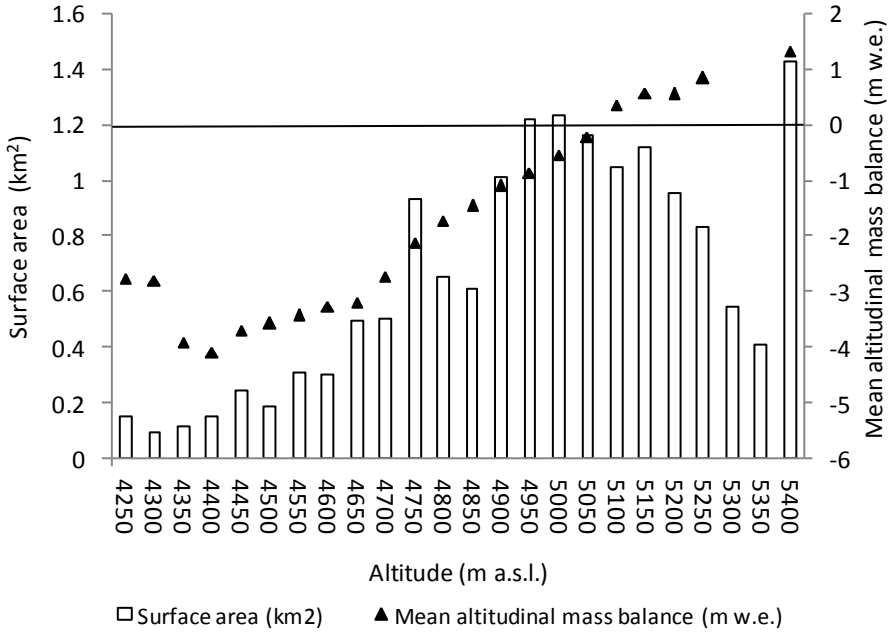

559

560 Figure 3

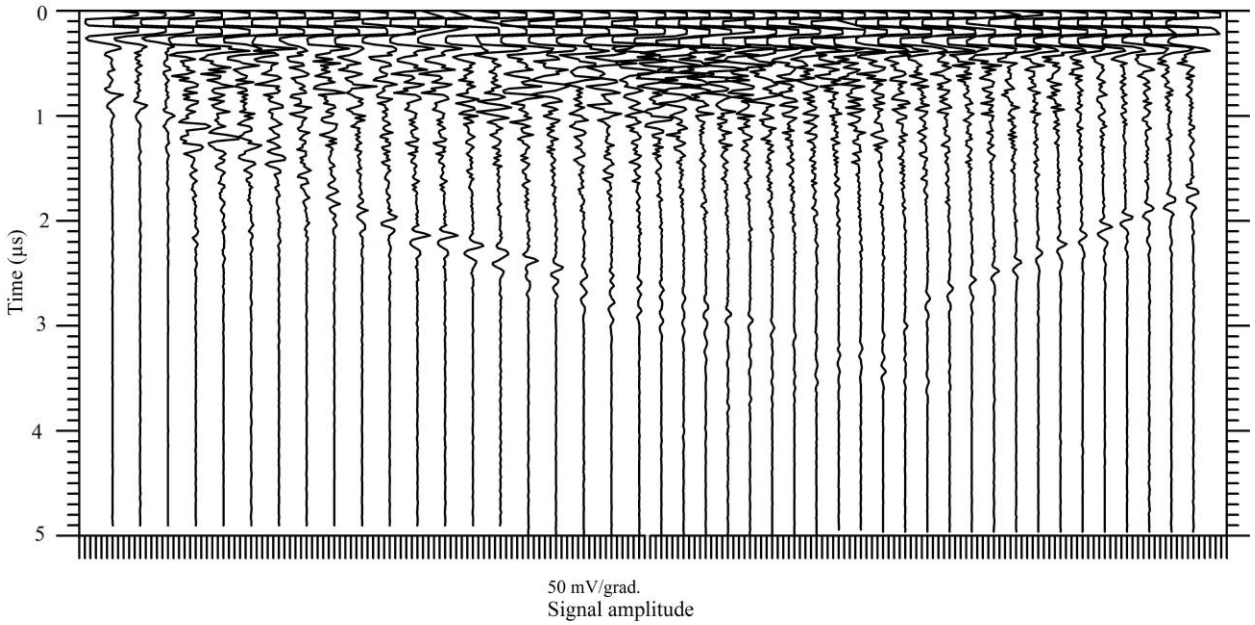

561

562 Figure 4

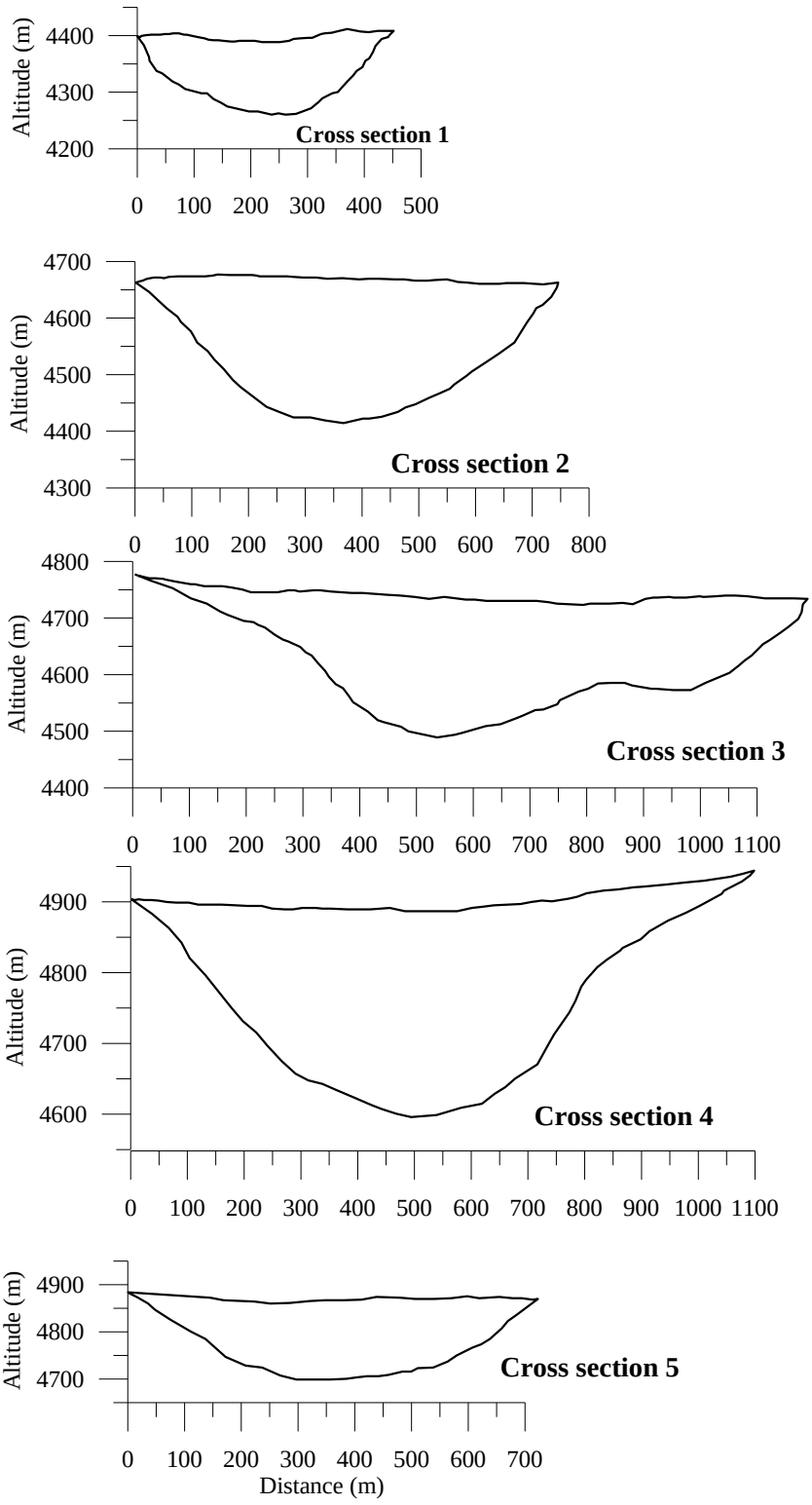

563

564 Figure 5

565

566

567

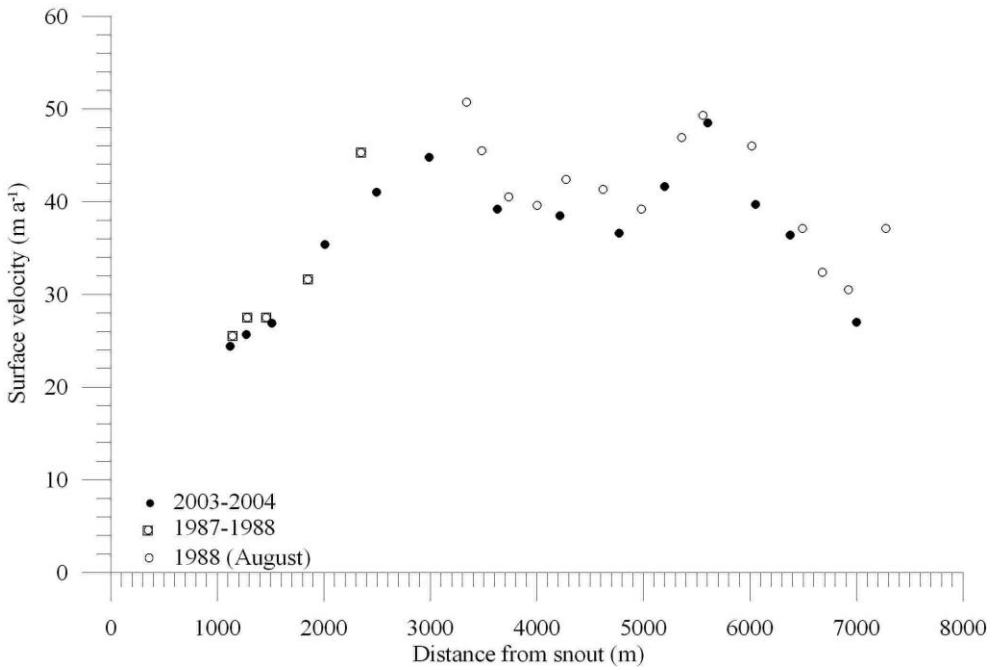

568

569 Figure 6

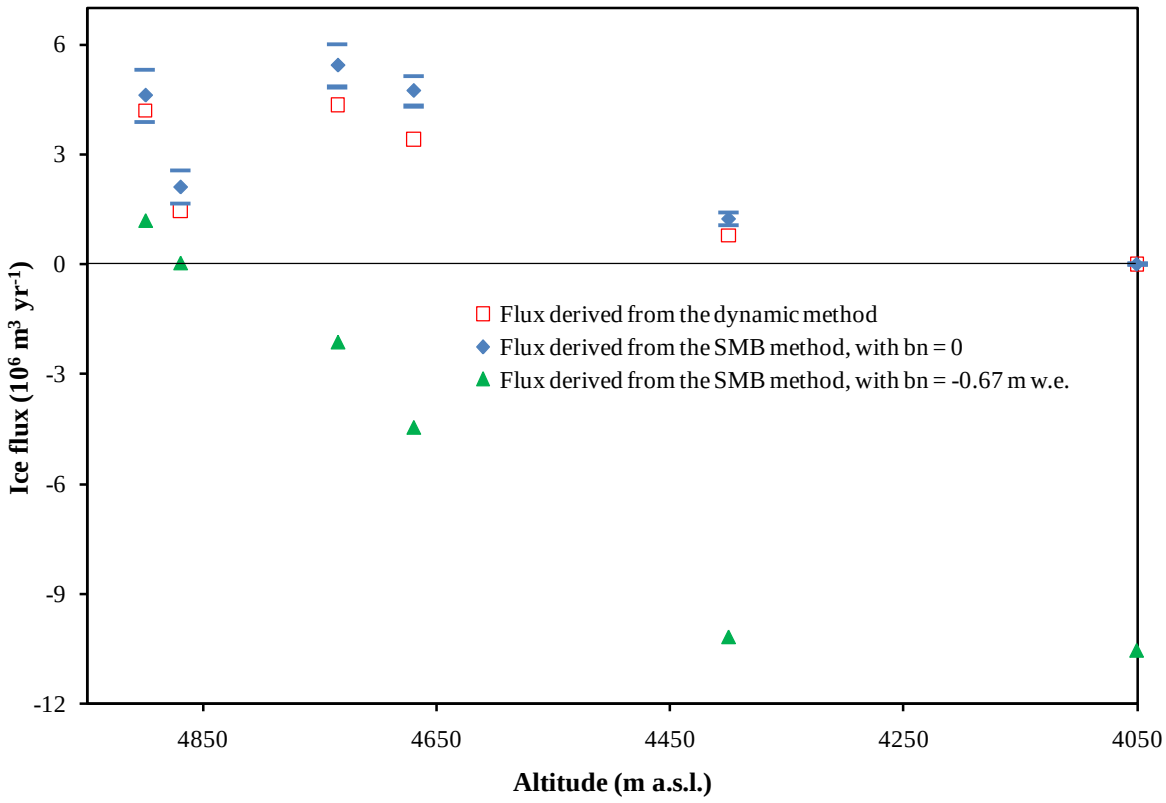

570

571 Figure 7

572

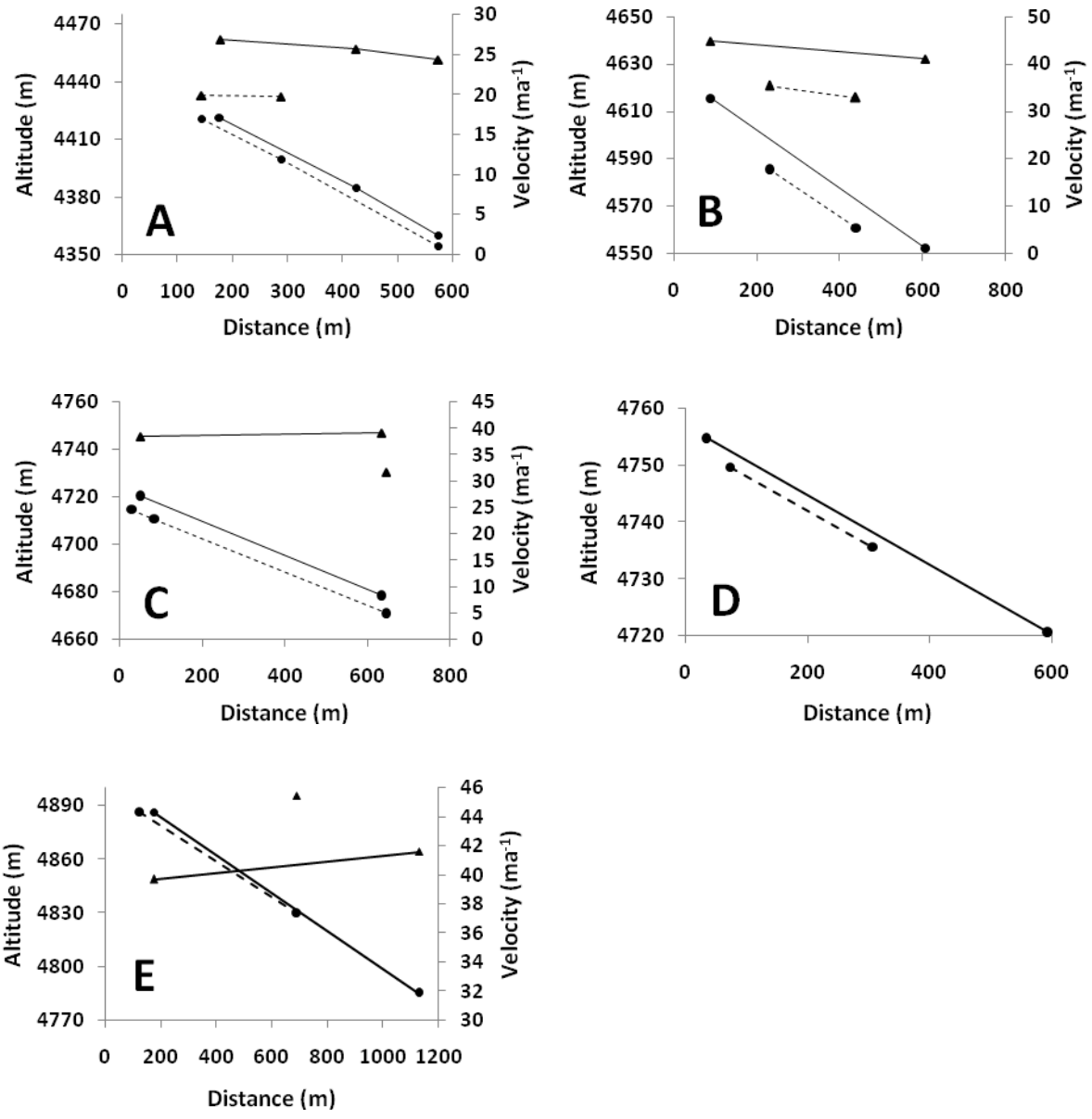

Figure 8